https://doi.org/10.1016/j.optlaseng.2017.10.006

Multipurpose, dual-mode imaging in the 3–5 µm range (MWIR) for artwork diagnostics: a systematic approach

Claudia Daffara[a], Simone Parisotto[b], Dario Ambrosini[c]

[a] *Dept. of Computer Science, University of Verona, Strada le Grazie 15, 37134, Verona, Italy*
[b] *CCA, Wilberforce Road, CB3 0WA, University of Cambridge, UK*
[c] *DIIIE, University of L'Aquila, P.le Pontieri 1, 67100, L'Aquila, Italy*

Abstract

We present a multi-purpose, dual-mode imaging method in the Mid-Wavelength Infrared (MWIR) range (from 3 µm to 5 µm) for a more efficient nondestructive analysis of artworks. Using a setup based on a MWIR thermal camera and multiple radiation sources, two radiometric image datasets are acquired in different acquisition modalities, the image in quasi-reflectance mode (TQR) and the thermal sequence in emission mode. Here, the advantages are: the complementarity of the information; the use of the quasi-reflectance map for calculating the emissivity map; the use of TQR map for a referentiation to the visible of the thermographic images. The concept of the method is presented, the practical feasibility is demonstrated through a custom imaging setup, the potentiality for the nondestructive analysis is shown on a notable application to cultural heritage. The method has been used as experimental tool in support of the restoration of the mural painting "Monocromo" by Leonardo da Vinci. Feedback from the operators and a comparison with some conventional diagnostic techniques is also given to underline the novelty and potentiality of the method.

Keywords: Thermal Quasi-Reflectography, thermography, nondestructive testing, artwork diagnostics

---

1. Introduction

Optical methods are excellent tools in metrology and diagnostics [1, 2]. The main features of these techniques, namely the non-contact approach, the flexibility and the full-field measurement, make them very well suited to artwork diagnostics. In particular, the full-field measurement was a key factor for their success and “imaging methods” are becoming more and more important, thanks to the rapid development of acquisition devices and image-processing algorithms and hardware. This impressive development led to the introduction and optimization of optical diagnostic techniques, both qualitative and quantitative [3, 4, 5, 6, 7, 8, 9, 10, 11], and to the wide diffusion of imaging investigative tools in the multidisciplinary field of cultural heritage, on which image-related sciences have a great impact [12, 13].

Infrared (IR) imaging is widely used in nondestructive analysis of paintings as it allows a non-contact and wide-field inspection in situ of their multi-layered features, namely the painting support, the pictorial layers, and the surface layers. Notable techniques are IR reflectography, which exploits the low scattering of the IR wavelengths up to 2.5 µm across the pictorial layers for imaging the features below the surface [14, 15] (e.g. preparatory drawings and repaintings), and IR thermography in the Long-Wavelength Infrared (LWIR) range (from 8 µm to 12 µm), which exploits the thermal contrast at the object surface induced by heat waves propagation for retrieving information about the deep structures [16, 17] (e.g. internal defects and/or lack of homogeneity). Given the complexity of artwork's materials and stratigraphy, a comprehensive diagnostics usually requires a multi-technique approach; thus, for example, thermography can be coupled to holography [18] or to reflectography [19] and imaging in different IR bands proved useful [20]. Specific imaging methods can be tailored to extract information from the different matter-radiation interaction properties of the layers. The thermal quasi-reflectography (TQR) approach [21] takes full advantage of the surface-interacting capability of the Mid-Wavelength Infrared (MWIR) wavelengths (from 3 µm to 5 µm) for imaging the pictorial layer in frescoes, where conventional IR reflectography is not effective, allowing the detection of features that are not imaged with traditional methods.

In this work a procedure, based on TQR, is proposed for IR diagnostics exploiting dual-mode acquisition in the MWIR range.

The paper is organized as follows: in Section 2 a schematic description of the proposed diagnostic procedure is given. Section 3 is devoted to the illustration of the basic features of TQR integrated in a dual-mode setup. In Section 4 the proposed procedure is treated in detail. In Section 5 the effectiveness of the procedure for the non-destructive analysis of mural paintings is shown in an exemplar case study: the notable restoration of the mural by Leonardo da Vinci of “Sala delle Asse” in the Sforza Castle in Milan, Italy [22]. Feedback from cultural heritage operators and comparisons with traditional diagnostic tools are also given to underline the novelty of the method.

2. Multipurpose, dual-mode MWIR imaging in a nutshell

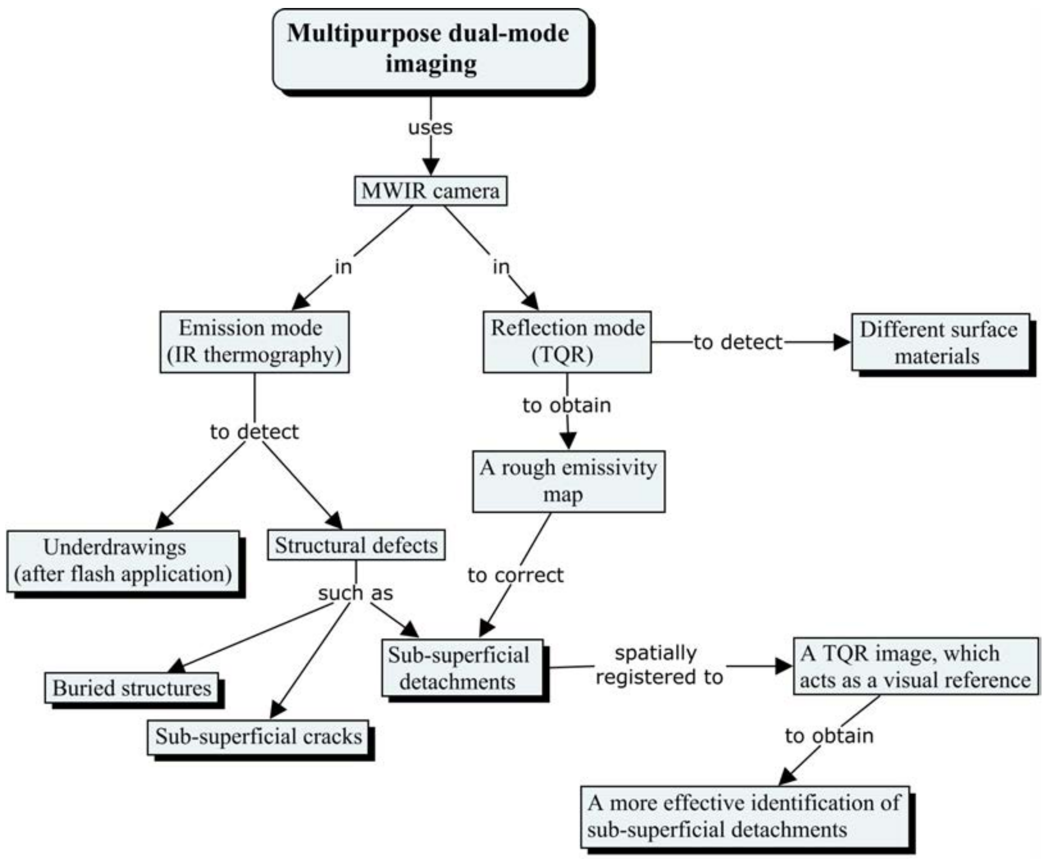

Figure 1: Schematic description of multipurpose dual-mode imaging.

The main concepts of the proposed dual-mode procedure are summarized in Figure 1. Using a setup based on a thermal camera and multiple radiation sources, two radiometric image datasets are acquired: the image in quasi-reflectography modality and the thermal sequence in emission modality. The dual-mode thermal stack is integrated to gain information.

The detection of structural defects by IR thermography is well described in literature [16]. Regarding the possibility to discover underdrawings, IR thermography after flash application [17] is not ideal: because of the low resolution of IR cameras, a dedicated equipment results in a better choice [15, 19]. However, as all the measurements described in Figure 1 are taken by the same recording device, images are spatially aligned and image fusion could be easily accomplished. In the following, the focus is on a full exploitation of TQR potentialities and on the detection of sub-superficial detachments by IR thermography powered by TQR results.

3. The TQR imaging technique integrated in a dual-mode setup

The core of the TQR imaging modality is the observation that an object with constant emissivity at room temperature has a very low emission in the MWIR band; if the surface temperature is 293 K, it emits about 1% of its thermal energy in the 3 µm to 5 µm range, as follows by the in-band Plank radiant exitance. Therefore, by sending MWIR radiation, properly matched with the thermal camera, and limiting any heating of the surface object, the acquired signal is dominated by the reflected radiation. As shown in [21], TQR imaging has the key feature to reveal details not detectable by conventional techniques.

Figure 2: Dual-mode imaging setup.

In Figure 2, a sketch of the dual-mode acquisition setup is given. A single thermal camera (geometry and optical configuration are fixed) is used for recording dataset both in emission mode and in reflection mode. The system employs multiple excitation sources. The heating sources, used for the thermal stimulus in emission mode measurements, are two quartz tungsten halogen lamps (1250 W). To prevent the transient cool down effect of the sources, a shutter has been applied after their switch off. In the present setup, the shuttering is mandatory; in fact, the residual heat of the high temperature halogen bulb matches the spectral response of the MWIR sensor. This is of particular importance when inspecting painted surfaces that are not high in emissivity: indeed, the transient lamp cool down signal, reflected back, could dominate or affect the recorded signal in thermal inspection [23].

The non-heating sources, used for reflection mode measurements, are custom designed as detailed in the following section.

3.1. TQR sources

The ideal TQR source should:

- exhibit a large, stable and smooth spectrum in the MWIR range;
- be capable of providing uniform irradiation over a large area, (e.g. FOV of 1 sqmt), thus enabling effective field measurements; exhibit a step-like emission, with rapid heat-up and cool-down;
- induce a heating on the target surface as small as possible. This is safe for artworks and a key issue in TQR to limit spurious contributions due to emission.

Since no source with these features is available in the market, it was specifically designed following [24]. The spectrum was modelled in grey-body approximation starting from the temperature and emissivity of filament, the transmission of the envelope, plus the emission of the envelope. Wien peak matches the MWIR in the range of temperature from 575 K to 975 K. This custom source was implemented starting from quartz elements with iron-chrome aluminium wire, which emit a large amount of MWIR, and polished aluminium reflectors. The elements were equipped with a thermocouple for monitoring the surface temperature. A suitable sapphire IR window was used to match MWIR band and to cut off unwanted thermal radiation. The system was controlled in power to maintain the same working temperature for the lamps. In the practice of TQR measurements, the emission of the MWIR source is then fine-tuned to the MWIR camera by optimizing the overall response on a lambertian certified reflectance target in-scene.

3.2. TQR reflectance

The MWIR reflectance, defined as the ratio of the incident and reflected radiant flux in the MWIR, is obtained as TQR measurement relative to a in-scene standard of known reflectance value. If S is the TQR radiometric image, the TQR reflectance is calculated point-wisely for the sampled pixel ij as follows

$$R_{ij}^{\mathrm{TQR}} = R_{\mathrm{ref}} \frac{S_{ij}}{S_{\mathrm{ref}}} \tag{1}$$

where R_{ref} is the certified reflectance of the standard (averaged in the MWIR) and S_{ref} the TQR measurement of the standard (averaged TQR image). The map R^{TQR} is the in-band diffuse reflectance in the MWIR, integrated spectrally by accounting the overall system response and angularly in the view collecting factor. Later, the issue of the quasi-reflectance approximation in the measurement is discussed.

The use of full-field calibrating panels is not practicable for in situ measurements of wall paintings; in our setup a partial-field target of 2 inches size is adopted. This may cause the spatial inhomogeneity in the surface signal to still affect the calibration of reflectance values. This issue is addressed later.

4. Dual-mode MWIR imaging procedures

The diagnostics is performed using the acquisition setup shown in Figure 2. This setup gives, for each area, two spatially registered dataset: a MWIR image in the quasi-reflectography modality (TQR) and a thermal sequence, in the thermography modality, after long-pulse heat stimulus. The measurement workflow can be summarized as follows:

1. TQR sources ON: record two TQR images, one with and one without a calibration target in scene;
2. TQR sources OFF; [Wait];
3. Start recording the thermal sequence;
4. Heat sources ON;
5. Heat sources OFF: shutter the heat sources and record the cooling.

As previously said, in a TQR measurement the recorded signal is dominated by the reflected radiation. As the reflectivity values depend on the materials and on the surface structure, TQR is very effective in differentiating surface elements [21, 23, 24]. Figure 3 shows the TQR ability to detect different materials, binders and surface treatments in comparison to IR standard reflectography. Lines were drawn with red pigment using different techniques. Figure 4 shows an example of TQR application to a real artwork in situ.

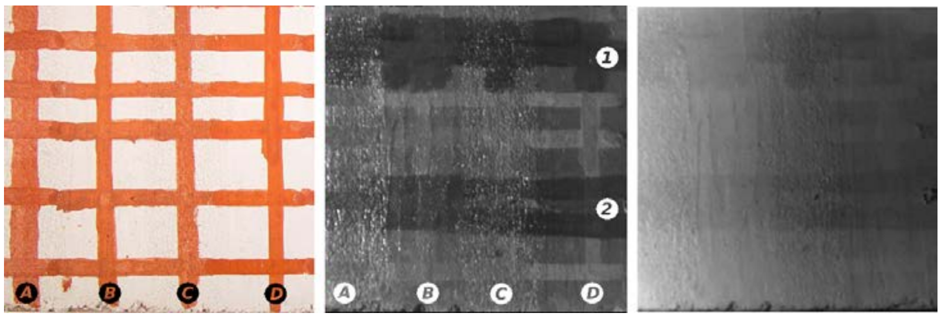

Figure 3: Fresco mock up: visible (left), TQR (center), IR (from 1.2 µm to 2.5 µm) reflectography (right). Lines were drawn with iron oxide pigments red and yellow ochre (color index PR 101 and PY 42) and different techniques. In columns: fresco (A); secco with no binder in smooth (B) and rough (C) surface; secco with limewash (D). In rows: different protective layers; vinyl coat (1) and rabbit-skin glue (2) have low MWIR reflectance. TQR is very sensitive to surface materials and roughness and differentiates pigment-binder-protective layers where IR reflectography is not effective.

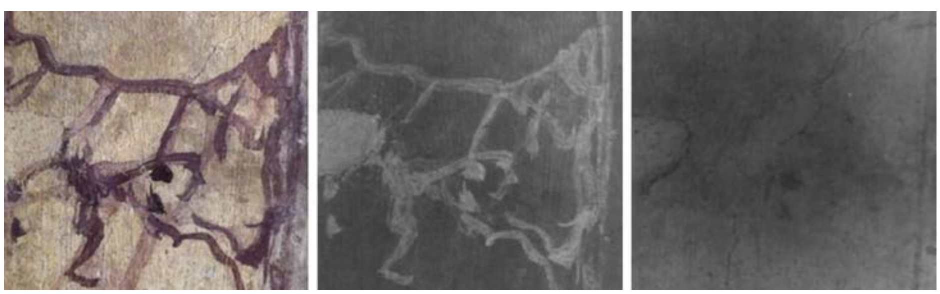

Figure 4: Detail of a 16th century Venetian fresco: visible (left), TQR (center), IR (from 1.2 µm to 2.5 µm) reflectography (right). TQR is capable to map pigments in ancient frescoes not detected by IR reflectography. The pigment with high TQR reflectance is iron oxide based, likely hematite.

4.1. TQR-based emissivity correction

The evaluation of the emissivity parameter is an important stage in IR thermography and it is a particularly critical issue when the surface is heterogeneous. Common methods are based on the use of reference emissivities (e.g. stickers, in thermal equilibrium with the surface) or on reference temperatures (e.g. contact measurements on the object). The TQR technique provides a noninvasive and non-contact alternative method to solve the emissivity problem in artwork diagnostics.

We assume the grey body approximation is valid, as in paintings diagnostics we usually deal with nonmetallic materials. Dependencies of emissivity from temperature range, wavelength, and angle are not relevant in the TQR setup. In our case, major parameters affecting the emissivity are the kind of material itself and the surface structure at micro-roughness level. Considering that the MWIR wavelengths do not penetrate painting layers, i.e. that surface reflectivity can be given as reflectance, and taking into account the Kirchhoff's law and energy conservation for the incident radiation on an opaque body, we obtain an approximate estimation of the surface emissivity ε, calculated point-wisely for the sampled pixel, from the values of the reflectance map measured with the quasi-reflectography technique (Equation (1))

$$\varepsilon_{ij} = 1 - R_{ij}^{\mathrm{TQR}} . \tag{2}$$

The Equation (2) is valid for an opaque surface under grey body approximation. An example of the emissivity correction based on TQR is reported in Section 5. The TQR and the thermography images are affected by kind of aberrations that lead to different spatial resolutions, i.e the thermographic image is more blurred than TQR due to the features of thermal diffusion. This issue is taken into account by proper filtering the TQR image before calculating the emissivity correction map in Equation (2).

4.2. TQR registration to visible orthophoto

The registration of multiple TQR images onto a visible reference orthophoto is another crucial stage. Indeed, when large portions of frescoes are under restoration, a comprehensive high resolution map of emissivities overlapped to the visible fresco would increase the quality of the analysis performed by restorers, allowing a multi-modal inspection of different regions far apart. Moreover, the benefits of a registered multi-modal dataset onto a reference orthophoto are not limited to the present days: future inspections with different techniques will also benefit of an aligned emissivity map.

Unfortunately, the imperfect positioning of the camera in front of the wall, due to space limitation of the environment, the need of using a mosaic of images, the different spatial resolution between the visible orthophoto and

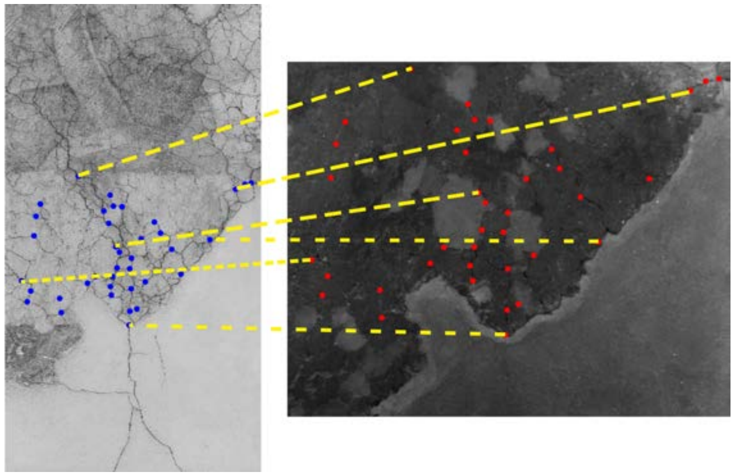

Figure 5: Registration of TQR frame onto orthophoto (and viceversa). In red the control points in TQR domain; in blue the control points in the orthophoto domain. The dashed yellow lines show the match between red and blue points.

TQR images, and the lack of control points helping the dual-mode registration, makes the projection problem challenging. However, some surface features (craquelures, stucco works, etc . . .) are still recognizable in both visible and TQR images and manual identification of craquelures-like defects can be used to drive the projective geometric transformation.

A procedure in Matlab, based on routines of the *Image Processing Toolbox*, was adopted: control points were first selected via the *Control Point Selection Tool* `cpselect.m`; then, the projective transformation was computed via the routine `fitgeotrans.m`, to estimate the transformation mapping the `moving` points (in TQR domain) onto the `fixed` points (in orthophoto domain), respectively the red and blue points in Figure 5. The only requirement for a correct estimate of the transformation map is a well-distributed covering of control points in the TQR frame.

Once that the transformation map is obtained, the inverse problem can be solved, i.e. given a rectangular frame in the TQR domain, a rectangular frame in the orthophoto domain can be obtained, in order to register the region of interest from the orthophoto onto the TQR frame.

In an ideal dual-mode imaging experiment, the transformation mapping TQR image onto the visible orthophoto will drive the same geometric registration of thermal images sampled at the same position in front of the wall onto the visible orthophoto. However, an automatic dual-mode craquelurebased registration process is left for future research.

4.3. Correction of TQR mosaic light inhomogeneities

The registered TQR mosaic could still suffer from nonuniform irradiance because of the in situ setup and the limited working space (e.g. the use of the partial field target and its incorrect displacement, the inaccurate position of lamps, the change of the environmental temperature conditions). In such situations, a post-processing intensity correction step would be desirable: a suitable procedure is based on a drift-diffusion filter [25, 26] able to remove constant shadows in images. Given a positive image f and a drift vector field of the type $\mathbf{d} = \nabla \log f$, the steady state u is given by the time evolution of the following linear equation

$$\begin{cases} \partial_t u = \Delta u - \operatorname{div}(\mathbf{d}u) \\ u(x,0) = f(x) \\ \langle \nabla u - \mathbf{d}u, \mathbf{n} \rangle = 0 \end{cases} \tag{3}$$

where $\langle \cdot , \cdot \rangle$ is the Euclidean scalar product and $\mathbf{n}$ is the outer normal vector on the boundary. Equation (3) has been named *osmosis filter*: indeed, when the drift vector field vanishes on *shadow edges*, then steady state solutions are shadowless, texture preserving, images. To sum up, such filter acts as a real osmotic process, balancing different concentrations (light inhomogeneities) through a semi-permeable membrane (shadow edges).

In our case, osmosis filter (3) is applied to a TQR mosaic made by many independent TQR samples, each one assumed affected by a constant light inhomogeneity and where TQR frame borders act as shadow edges. However, TQR mosaic of large size would slow down the post-processing so efficient numerical solver are needed for a fast in situ analysis [27]. The procedure adopted is based on Alternating Directional Implicit (ADI) splitting methods to split the finite difference matrix $\mathbf{A}$ of Equation (3) along the spatial directions, which are solved separately. Following [28], Additive Operator Splitting (AOS) and Multiplicative Operator Splitting (MOS) In detail, for every iteration k and time-step τ the AOS and MOS splitting methods read as

$$\mathbf{u}^{k+1} = \frac{1}{2} \sum_{n=1}^{2} \left(\mathbf{I} - 2\tau \mathbf{A}_n\right)^{-1} \mathbf{u}^k, \tag{AOS}$$

$$\mathbf{u}^{k+1} = \prod_{n=1}^{2} \left(\mathbf{I} - \tau \mathbf{A}_n\right)^{-1} \mathbf{u}^k, \tag{MOS}$$

which are stable for any τ and first-accurate in time. Also, standard properties of the continuous osmosis equations hold for the discretized model: the Average Gray Value Conservation (AVG), the preservation of the positivity and the convergence to a unique steady state. The importance of the AVG preservation in real applications is emphasised since no information is lost when osmosis filter is applied iteratively.

4.4. The quasi-reflectography measurement

The systematic contribution of the surface thermal emission in the quasi-reflectography approximation is analysed in order to evaluate the accuracy of the measured reflectance R^{TQR}. For a given object temperature T_{obj} the influence of the radiation emitted by a surface element increases when its reflectance R decreases.

For the short measurement distance typical of the TQR setup ($\sim$1 m) the attenuation due to ambient atmosphere is negligible; the radiometric chain for TQR imaging that gives the radiation power incident on the detector Φ_{det} in terms of the contributions reflected and emitted by the object is

$$\Phi_{\text{det}} = R\Phi_{\text{src}} + (1 - R)\Phi^{\text{bb}}(T_{\text{obj}}) \tag{4}$$

with Φ_{src} the radiant power of the source incident on the surface and $\Phi^{\text{bb}}(T_{\text{obj}})$ the blackbody radiant power at object temperature. All the contributions include the dependences on the acquisition setup geometry and camera properties, which are fixed during the measurements; the detector signal is then integrated over the wavelength in the MWIR band, accounting for the spectral dependence of the specific system response and source. The calibrated reflectance can be obtained after measuring the detector response on the reference reflectance target; supposing the target and the object at the same temperature (i.e., avoiding any heating by the TQR source) and translating in signal of the detector S, the actual point-wise reflectance is given by the following

$$R_{ij} = R_{\mathrm{ref}}\,\frac{S_{ij} - S_{ij}^{\mathrm{bb}}(T_{\mathrm{obj}})}{S_{\mathrm{ref}} - S_{ij}^{\mathrm{bb}}(T_{\mathrm{obj}})}\,. \tag{5}$$

In the quasi-reflectance measurement the relative signal “error” due to the emitted radiation, in regard to an ideal reflectance measurement, is

$$\frac{\Delta\Phi}{\Phi} = \frac{\Phi_{\mathrm{det}} - R\Phi_{\mathrm{src}}}{R\Phi_{\mathrm{src}}} = \frac{1-R}{R}\,\frac{\Phi^{\mathrm{bb}}(T_{\mathrm{obj}})}{\Phi_{\mathrm{src}}} \tag{6}$$

which provides the accuracy of the TQR-measured reflectance. For a blackbody source picked at 4 µm ($T = 724\,\mathrm{K}$) and range of temperatures safe for the artwork, we have for the MWIR in-band quantity $\Phi_{\mathrm{obj}}^{\mathrm{bb}}/\Phi_{\mathrm{src}}{\sim}10^{-3}$ (Figure 6). The fraction of reflected radiation, i.e. the first term in Equation (4), with regard to the total one received by the detector is depicted in Figure 7. The graphic shows that in the range of working temperature the measurement is performed in a very good reflectance approximation for different values of the object reflectance (nonmetallic materials) and that such approximation is stable under small variation of the object temperature.

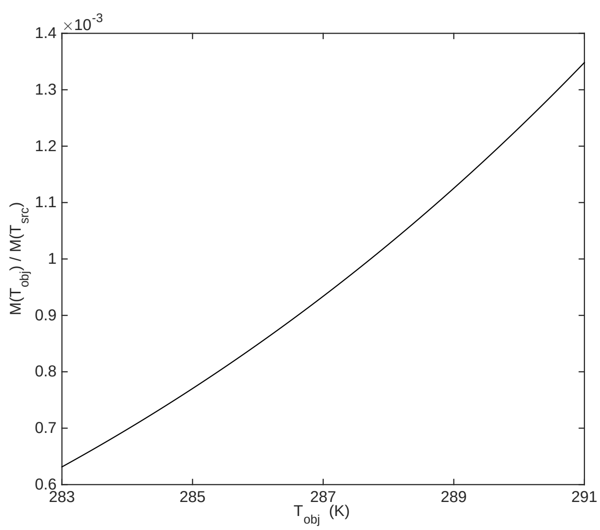

Figure 6: The quantity $\Phi_{\mathrm{obj}}^{\mathrm{bb}}/\Phi_{\mathrm{src}}$ computed as ratio of in-band blackbody exitance of different object temperatures and a MWIR source nominally picked at 4 µm ($T = 724\,\mathrm{K}$). At a room temperature ($T_{\mathrm{obj}} = 293\,\mathrm{K}$) $\Phi_{\mathrm{obj}}^{\mathrm{bb}}/\Phi_{\mathrm{src}} = 9.3 \times 10^{-4}$.

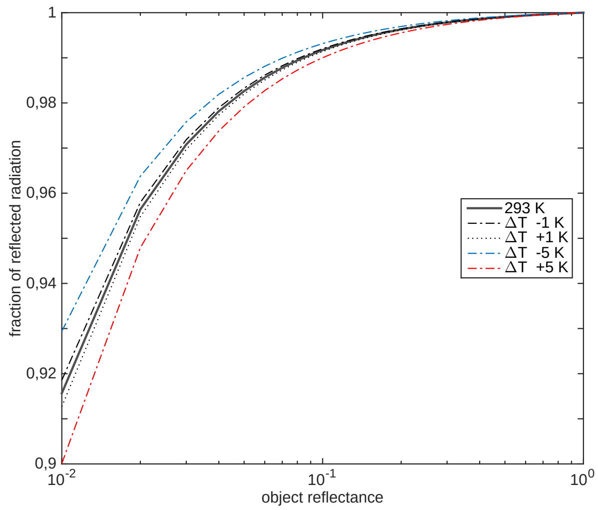

Figure 7: Fraction of the radiation reflected by the object in regard to total incident on the detector for different object reflectance at different object temperatures (semilog plot). Small variations of 1 degree that may occur during in situ measurement are not critical.

5. Experimental results and discussion

Dual-mode imaging in the MWIR was applied to support the restoration intervention of the mural painting "Monocromo" by Leonardo da Vinci (Figure 8) in the period 2015-2016, with regard to the treatment of the surface materials and the consolidation of the subsurface detaches [22]. Spatial resolution, full-field screening, and referentiation to the visible were asked by the operators as mandatory factors for the effectiveness of the analysis.

The acquisition geometry was setup to obtain a sub-millimetric spatial resolution ($\sim$0.5 mm).

Dual-mode imaging was performed by FLIR X6540sc camera, equipped with a cooled InSb detector (640$\times$512 array, 15 µm pixel pitch) with MWIR sensitivity and a NEDT of 20 mK. The lens was a 25mm with a FOV of $22° \times 17°$. The native ResearchIR Max 4 software was used in the recording phase. Beside high sensitivity and accuracy, the camera enables full access to the radiometric data at detector level. The reference standard for the calibration of the TQR reflectance was an Infragold diffuse target by Labsphere of 2 inches size. The thermal sequence was acquired at 120 Hz after a 120 s long-pulse heat stimulus.

Figure 8: Dual-mode measurement on Leonardo mural painting “Monocromo”, Sforza Castle, Milan.

The effectiveness of TQR imaging for the surface deterioration study is shown in Figure 9. In this case, abundant crystallized salts (mainly sulphate and nitrate salts) are detected thanks to the high MWIR reflectance. This clear map of the salt patinas was not provided by the more traditional imaging technique based on UV light. Surface treatments from past intervention are well detected. Figure 10 reports an example of dual-mode imaging in the MWIR showing the complementarity of the TQR and thermographic measurement. In this case, the TQR detects the different surface patches (stucco), while the thermography discriminates the presence of subsurface consolidant (cement) from the cooling behaviour.

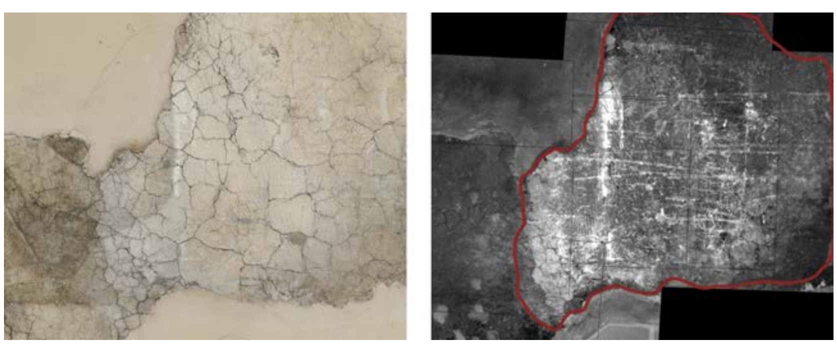

Figure 9: A fresco detail; visible and TQR image (mosaic), mapping the surface salt decay. The region with the crystallization is outlined in red.

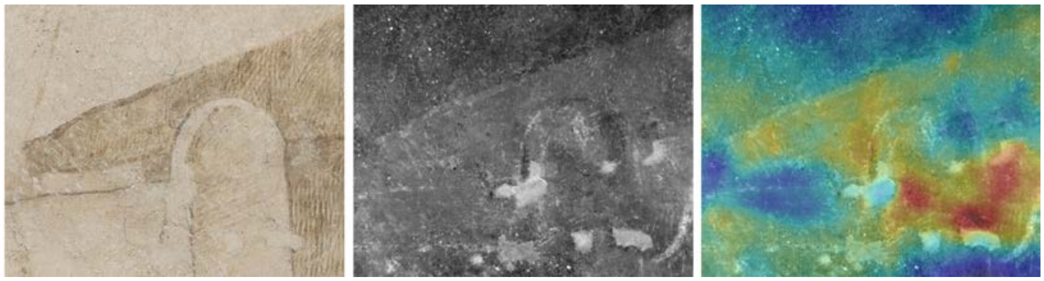

Figure 10: Example of dual-mode imaging for diagnostics in a fresco detail: visible (left); TQR measurement (center); alpha fusion image between TQR and thermogram after the lamps switch-off (right).

Figure 11 depicts the TQR workflow for a frame acquired on the Leonardo painting according to Sections 3 and 4. The result is a spatially aligned dataset with the TQR calibrated reflectance, the emissivity map, and the visibile image of the corresponding region. Figure 12 shows as result the mosaic of emissivity obtained from three TQR frames, computed by applying the image osmosis filter with AOS splitting method. As shown in the results in Figure 13, the mosaic of the thermographic frames is obtained from the TQR allowing to solve in precise way the crucial issue of referencing thermography to the visible. In this specific work, the dual-mode MWIR technique has allowed to produce a considerably large map of the Leonardo wall with surface and subsurface features referenced at sub-millimetric accuracy that represented a valuable tool for the operators during the intervention.

6. Conclusions

This paper was devoted to a systematic approach of a multipurpose, dual-mode imaging in the MWIR (3 µm to 5 µm) range, in which the features of IR thermography enrich the powerfulness of thermal quasi-reflectography (TQR).

The main advantages of the proposed procedure are:

- the acquisition of complementary surface and sub-surface information with an imaging setup based on a single camera;
- the use of TQR map for registering the thermographic images, which are “blurred” due to heat diffusion, onto the visible images;

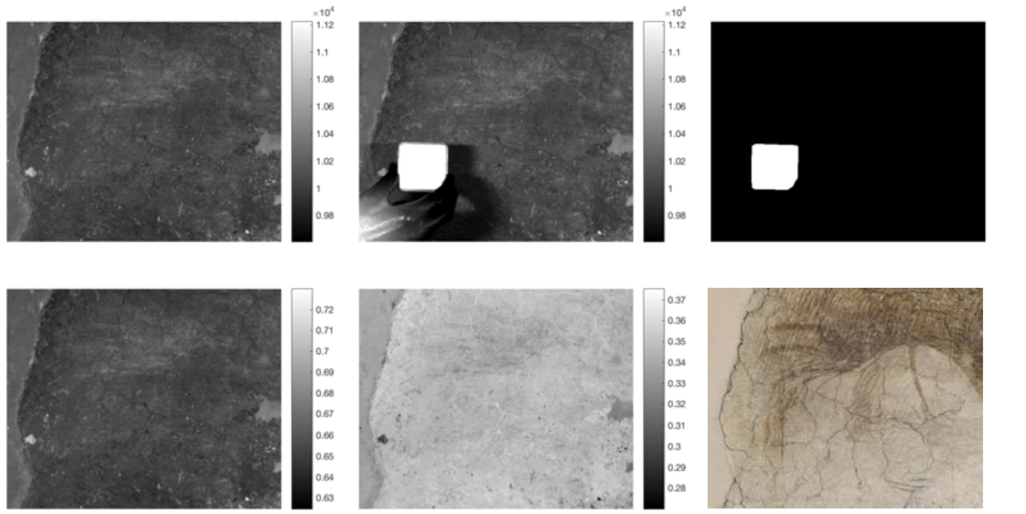

Figure 11: TQR workflow for the single frame: TQR raw radiometric image (top-left); TQR golden target in-scene (top-middle); target segmentation (top-right). TQR calibrated reflectance (bottom-left); emissivity map obtained from TQR (bottom-middle); visible orthophoto (bottom-right) spatially aligned to TQR. For visualization purposes only, the colormap has been fixed to the data range without the target in figure top-left and top-middle.

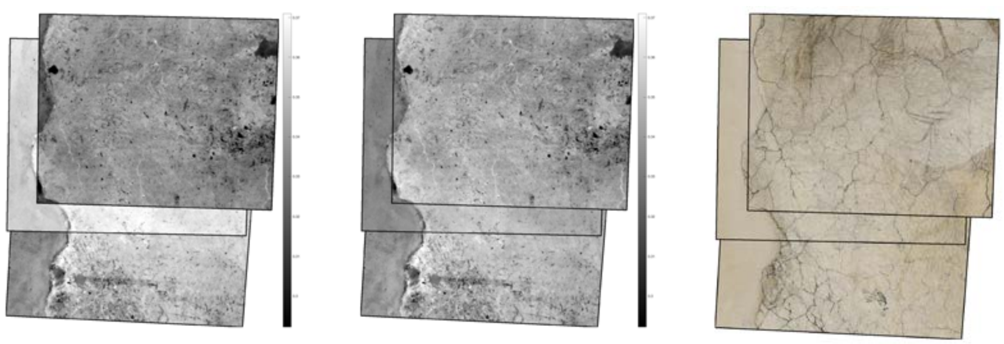

Figure 12: From left to right: mosaic of three emissivity frames; light corrected emissivity mosaic following [28]; visible orthophoto.

- the possible use of the quasi-reflectance map, acquired by the TQR modality, for a simple yet effective emissivity correction in support of the thermographic analysis.

TQR performance was enhanced by designing a custom source and by

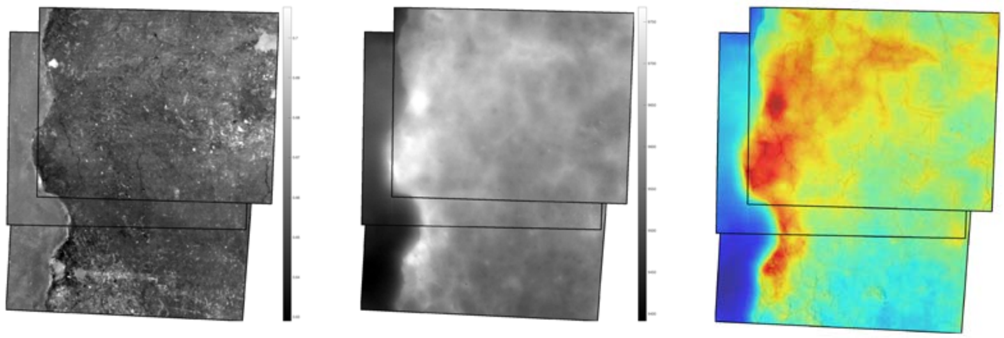

Figure 13: Example of TQR-thermal integration for defect detection on mosaic in Figure 12: TQR reflectance mosaic (left); radiometric thermal measurement after switching off the lamps (center); alphaColor image between radiometric thermal measurement and visible orthophoto (right) showing the precise localization of the detachment. Left and central mosaic have been post-processed as in [28] for light inhomogeneity correction.

defining suitable measurement procedures.

Dual-mode imaging was validated on a notable case study: the restoration of the mural painting by Leonardo da Vinci of “Sala delle Asse” in the Sforza Castle in Milan, Italy. The method was capable to provide high resolution maps of the painting surface as well as maps of the sub-surface defects referentiated to the visible by the TQR investigation. The results were validated in situ by expert restorers, which confirmed the uniqueness and importance of the proposed diagnostic method.

Acknowledgements

The authors are grateful to Eng. Francesco Messa (*FLIR Systems*) for the support in the thermal measurements and to the restorer Paola Ilaria Mariotti (*Opificio delle Pietre Dure*) for the validation of the results. The diagnostics was supported by Dr. Francesca Tasso (*Soprintendenza* of Castello Sforzesco).

SP acknowledges the UK EPSRC grant EP/L016516/1 for the University of Cambridge DTC, the Cambridge Centre for Analysis.

Data Statement

The data leading to this publication are sensitive; restricted access is subjected to the approval of Castello Sforzesco’s administration “Soprintendenza Castello, Musei Archeologici e Musei Storici”, Milan.

References

[1] Yoshizawa T, editor. Handbook of optical metrology.Boca Raton: CRC Press; 2008.

[2] Rastogi P, editor. Digital optical measurement - Techniques and applications. Boston: Artech House; 2015.

[3] Paoletti D, Schirripa Spagnolo G. IV Interferometric Methods for Artwork Diagnostics. In: Wolf E, editor. Progress in Optics 35, Amsterdam: Elsevier; 1996, p. 197–255.

[4] Schirripa Spagnolo G, Ambrosini D, Paoletti D. An NDT electro-optic system for mosaics investigations. J Cult Herit 2003; 4:369-76.

[5] Ambrosini D, Paoletti D. Holographic and speckle methods for the analysis of panel paintings. Developments since the early 1970s. Stud in Cons 2004; 49 (sup1): 38–48.

[6] Hinsch KD, Glker G, Helmers H. Checkup for aging artwork Optical tools to monitor mechanical behaviour. Opt Lasers Eng 2007; 45: 578–88.

[7] Fotakis C, Anglos D, Zafiropulos V, Georgiou S, Tornari V. Lasers in the preservation of cultural heritage: principles and applications. New York: Taylor & Francis; 2007.

[8] Theodorakeas P, Ibarra-Castanedo C, Sfarra S, Avdelidis NP, Koui M, Maldague X, Paoletti D, Ambrosini D. NDT inspection of plastered mosaics by means of transient thermography and holographic interferometry. NDT & E Int 2012; 47: 150–6.

[9] Targowski P, Iwanicka M. (2012). Optical coherence tomography: its role in the non-invasive structural examination and conservation of cultural heritage objects a review. Appl Phys A 2012; 106: 265–77.

[10] Liang H. Advances in multispectral and hyperspectral imaging for archaeology and art conservation. Appl Phys A 2012; 106: 309–23.

[11] Alfeld M, Broekaert JA. Mobile depth profiling and sub-surface imaging techniques for historical paintingsa review. Spectrochim Acta Part B At Spectrosc 2013; 88: 211–30.

[12] Cappellini V, Maitre H, Pitas I, Piva A, editors. Special issue on Image processing for cultural heritage. IEEE Trans Image Process 2004; 13: 273–448.

[13] Chetouani A, Erdmann R, Picard D, Stanco F, editors. Special section on Image processing for cultural heritage. J Electron Imaging 2017; 26: 011001–29.

[14] van Asperen de Boer JRJ. Infrared reflectography - a method for examination of paintings. Appl Opt 1968; 7: 1711–14.

[15] Daffara C, Fontana R. Multispectral infrared reflectography to differentiate features in paintings. Microsc Microanal 2011; 17: 691-95.

[16] Maldague XPV. Theory and practice of infrared technology for nondestructive testing. New York: Wiley-Interscience; 2001.

[17] Gavrilov D, Maev RGr, Almond DP. (2014) A review of imaging methods in analysis of works of art: thermographic imaging method in art analysis. Can J Phys 2014; 92: 341–64.

[18] Ibarra-Castanedo C, Sfarra S, Ambrosini D, Paoletti D, Bendada A, Maldague XPV. Diagnostics of panel paintings using holographic interferometry and pulsed thermography. Quant Infrared Thermogr J 2010; 7: 85–114.

[19] Ambrosini D, Daffara C, Di Biase R, Paoletti D, Pezzati L, Bellucci R, Bettini F. Integrated reflectography and thermography for wooden paintings diagnostics. J Cult Herit 2010; 11: 196-204.

[20] Daffara C, Pezzati L, Ambrosini D, Paoletti D, Di Biase R, Mariotti PI, Frosinini C. Wide-band IR imaging in the NIR-MIR-FIR regions for in-situ analysis of frescoes. Proc. SPIE 2011; 8084: 808406.

[21] Daffara C, Ambrosini D, Pezzati L, Paoletti D. Thermal quasi-reflectography: a new imaging tool in art conservation. Opt Expr 2012; 20: 14746–53.

[22] Palazzo C, Tasso F, editors. Leonardo da Vinci. The Sala delle Asse of the Sforza Castle. Diagnosting Testing and Restoration of the Monochrome. Milano: Silvana Editoriale Spa; 2017.

[23] Daffara C, Parisotto S, Mariotti PI. Mid-infrared thermal imaging for an effective mapping of surface materials and sub-surface detachments in mural paintings: integration of thermography and thermal quasi-reflectography. Proc SPIE 2015; 9527: 95270I.

[24] Daffara C, Ambrosini D, Pezzati L, Marchioro G. Thermal quasi-reflectography (TQR): current research and potential applications. Proc. SPIE 2013; 8790: 87900S.

[25] Vogel O, Hagenburg K, Weickert J, Setzer S. A Fully Discrete Theory for Linear Osmosis Filtering. In: Kuijper A, Bredies K, Pock T, Bischof H (eds) Scale Space and Variational Methods in Computer Vision. SSVM 2013. Lecture Notes in Computer Science 2013; 7893. Springer, Berlin, Heidelberg.

[26] Weickert J, Hagenburg K, Breu M, Vogel O. Linear Osmosis Models for Visual Computing. In: Heyden A, Kahl F, Olsson C, Oskarsson M, Tai XC (eds) Energy Minimization Methods in Computer Vision and Pattern Recognition. EMMCVPR 2013. Lecture Notes in Computer Science 2013; 8081. Springer, Berlin, Heidelberg.

[27] Calatroni L, Estatico C, Garibaldi N, Parisotto S. Alternating Direction Implicit (ADI) schemes for a PDE-based image osmosis model. arXiv preprint 2017; 1703.04453.

[28] Parisotto S, Calatroni L and Daffara C. Efficient Osmosis Filtering of Thermal-Quasi Reflectography Images for Cultural Heritage, arXiv preprint 2017; 1704.04052.